

## Enhancement the photocatalytic activity of Zinc Oxide surface by combination with Functionalized and non-Functionalized Activated Carbon

Eman J. Mohammad<sup>1</sup>, Abbas J. Lafta<sup>1\*</sup>,  
Salih H. Kahdem<sup>1</sup>, Ayad F. Alkaim<sup>2</sup>

<sup>1</sup> Chemistry Department, College of Science, University of Babylon, Hilla, Iraq, 51002.

<sup>2</sup> Chemistry Department, College of Science for Women, University of Babylon, Hilla, Iraq, 51002.

**Abstract :** The current study, describes synthesis and functionalization of activated carbon that is derived from Iraqi date palm seeds and its combination with zinc oxide nanoparticles to yield activated carbon/zinc oxide (AC/ZnO), and functionalized activated carbon /zinc oxide (FAC/ZnO). These materials were characterized using powder X-rays diffraction (PXRD), Fourier transform infrared spectroscopy (FTIR) and specific surface area (BET). The photocatalytic activity of these materials was investigated by following removal of Celestin blue b dye (CBB) from textile wastewaters. Besides that, impact of different reaction parameters were investigated such as effect of the temperature, pH, contact time, as well as dosage effect. Activation energy for dye removal was calculated according to Arrhenius equation and it was around 27.71 kJ/mol. It was found that, the photocatalytic activity of these materials towards dyes removal was as follows: AC/ZnO > FAC/ZnO > ZnO.

**Keywords :** Activated carbon, Activated carbon/ZnO, Textile dye removal over activated carbon., Adsorption of Celestin blue b, functionalized activated carbon.

### Introduction

In the last few decades, synthetic dyes are important source for pollution especially in the industrial wastewaters. These are contributed in many types of industries and different human activities such as textile industries, food, paper, ink and photographic processes<sup>1-3</sup>. Among all these sources of pollution with dyes, textile dyes seem to be main source of pollution, this arises from high colored density in wastewaters effluent, high toxicity and aromatic rigid structure of vast majority of these dyes. This rigid aromatic structure makes these dyes to be stable under normal conditions and are not biodegradable<sup>4,5</sup>. In addition to that, these dyes have massive effects on human health, plants, air, water and soil. For all these reasons, treatment of these dyes from industrial wastewaters becomes a big challenge. Currently, there are several methods are applied in dealing with this issue. These including adsorption phenomenon, aerobic and anaerobic degradation, coagulation and precipitation<sup>6</sup>. However, these processes are not too efficient in treatment in dye removal from wastewaters besides that they may transfer polluted dyes from one form to another or in some cases they can react with ambient conditions to yield further toxic materials as these methods don't afforded destructive fragmentation of these dyes<sup>7</sup>. In this context it becomes too necessary to search for alternative methods for dye treatment, this involves advanced oxidation processes (AOPs), photobleaching and heterogeneous photocatalytic processes<sup>8</sup>.

These alternative methods includes generation of reactive species such as hydroxyl radicals, peroxide and super oxide radicals. These radicals can participate in fully destructive of dye molecules into water and carbon dioxide as well as other inorganic materials<sup>9,10</sup>. Generally, the use of the later methods requires combination of this system with photocatalyst to provide a sufficient surface for dye molecules destruction. Currently, many photocatalyst are used in this field such as semiconductor photocatalysts like TiO<sub>2</sub>, ZnO, Fe<sub>3</sub>O<sub>4</sub>, CoO and V<sub>2</sub>O<sub>5</sub> and Cr<sub>2</sub>O<sub>3</sub><sup>11-14</sup>. Among wide range of these materials zinc oxide (ZnO) seems to be more efficient photocatalyst due to it excellent chemical and physical properties as well as its low cost, non-toxicity, and it can be recycled for further usage after just easy activation processes<sup>15</sup>. In spite of all these promising points, the main draw back with ZnO and other photocatalysts, is that the absorption of light with high efficiency in the UV region of the solar spectrum. Also they suffer from recombination reaction between conduction band electrons and valence band holes. The last process reduces the efficiency of the photocatalytic reaction considerably<sup>16,17</sup>. In order to reduce the rate of recombination reaction and improve the photocatalytic activity of zinc oxide and extend its photoresponse towards visible region of the solar spectrum. Many methods have been undertaken to modify its surface properties such as surface doping with traces of some dopants, surface sensitization and coupling with small band gap photocatalysts. In this context, combination of zinc oxide with other co-adsorbent with high surface area such as activated carbon can enhance its photocatalytic activity by providing large surface area and increasing charge separation between e<sup>-</sup><sub>CB</sub> and h<sup>+</sup><sub>VB</sub>, hence these species can diffuse into the surface and then react with pre-adsorbed redox species on the surface. However, synergistic effect between ZnO and AC particles can improve its photocatalytic activity. Until yet real mechanism for this process is not understood completely and it is believed that this effect may arise from the role of AC in wide separations of ZnO particles at the high surface area of AC<sup>18-20</sup>. In some case, negative effect on photocatalytic activity of ZnO when combination with ZnO may result from the role of AC particles on screening of photons of light away from active sites of the surface of ZnO<sup>21-22</sup>. On the other hand, functionalization of the AC surface can improve its surface properties by introducing variety of functional groups on the surface. These proposed functional groups can enhance surface properties of AC which can lead to improve catalytic properties of the binary system (AC/ZnO)<sup>23,24</sup>.

The current study involves synthesis of AC and its combination with ZnO to yield (AC/ZnO), also it would involve functionalization of AC and its combination with ZnO to yield (ACF/ZnO). The photocatalytic activity of these binary systems would be screening via following removal of Celestin blue b (CBB) from aqueous solution.

## Experimental part

### Used chemicals

In this study Celestin blue b dye (CBB) was used as a dye model, it has a molecular formula of C<sub>17</sub>H<sub>18</sub>ClN<sub>3</sub>O<sub>4</sub> and a molecular weight of 363.80g.mol<sup>-1</sup>. It was provided by Sigma Aldrich Company (80%). This dye was used as it provided without any further purification processes. The chemical structure of this dye is shown in Figure 1. Zinc oxide Zinc oxide that was used in this study was provided byFluka company (99.5%), its molecular formula is ZnO with a molar mass of 81.401 g/mol with a density of 5.606 g/cm<sup>3</sup> and has a melting point of 1975 °C with a bandgap energy of 3.37 eV<sup>(25)</sup>.

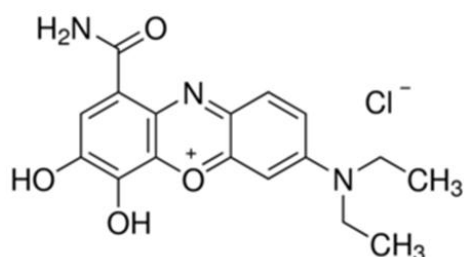


**Figure 1: Chemical structure of Celestine blue dye(CBB)**

### Synthesis of activated carbon

Synthesis and investigation of physical properties of activated carbon using Iraqi zahdi date palm seeds (IZDPS) using KOH as a chemical activator were reported in our previous published work<sup>26</sup>.

### Synthesis of binary system of AC/ZnO

A ratio of AC/ZnO composite (10%) was synthesized using a simple evaporation and drying process. According to this method, commercial ZnO was suspended in 100 mL of DW and sonicated for 30 minutes. In another flask, activated carbon was suspended in 20 mL of DW and sonicated for 15 minutes. Then AC solution was added to ZnO suspension with continuous stirring. The obtained mixture of a suspension containing AC and ZnO particles was heated at 80 °C until the complete evaporation of water. Then the obtained remaining composite was dried overnight in an oven at 100 °C to yield AC-ZnO composite<sup>27</sup>.

### Synthesis of the functionalized activated carbon

Synthesis of functionalized activated carbon (FAC) was prepared by suspending 500 mg of AC in 150 mL of distilled water in a 250 mL conical flask in a water bath shaker. To this suspension, 5 mL of concentrated HNO<sub>3</sub> was added and the mixture was stirred for two hours at room temperature. The AC and acid suspension was kept under stirring in a water bath at room temperature for 1 hr to open the agglomeration of the activated carbon and to anchor the acid solution uniformly on the carbon surface. After that, mixture was filtered off and the obtained solid was dried in an oven at 105 °C for two hours to yield FAC<sup>28</sup>. The synthesis of a composite of FAC and zinc oxide was prepared using the same above procedure that was applied in the synthesis of AC-ZnO to yield FAC-ZnO.

### Determination of surface area of activated carbons and its combination with ZnO

Specific surface area for AC and FAC, AC-ZnO and FAC-ZnO samples were investigated according to the procedure that was reported according to Saers, method<sup>29</sup>.

### Investigation of the composite of AC-ZnO and FAC-ZnO

A binary composite materials AC/ZnO and FAC/ZnO were investigated using powder X-ray diffraction (PXRD), Fourier transform infrared spectroscopy (FTIR) and specific surface area (BET).

### Photocatalytic experimental setup

Photocatalytic experiments were performed in a homemade photoreactor that is shown in Figure 2. All experiments were conducted using an aqueous solution of CBB dye (50 ppm, 30 mL) with suspension of a required mass of the used catalysts. Photocatalytic reactions were carried out under irradiation with UV light from a low pressure mercury lamp. In all cases, photocatalytic reactions were started after performing a dark reaction for each experiment to ensure reaching adsorption equilibrium for each run. Reaction progress was investigated by following the absorbance of the supernatant liquid of dye solution at 642 nm using UV-Vis Shimadzu 1650 PC-UV-visible Spectrometer photometer. The percentage of dye removal (R%) was conducted using the following relationship<sup>30</sup>.

$$R \% = \frac{C_i - C_f}{C_i} \times 100$$

whereas,  $C_i$  is the initial concentration of CBB dye,  $C_f$  is the final concentration of the dye after one hour adsorption process.

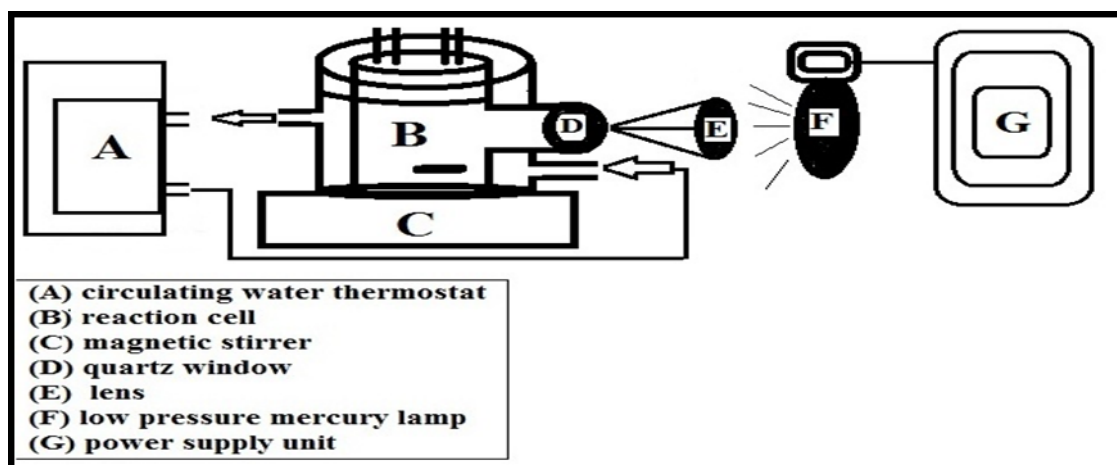


Figure 2: Photoreactor unit set up that was used to perform photocatalytic reactions in this study

## Results and discussion

### Specific surface area of the binary composite materials

The specific surface area of each of AC, FAC, AC-ZnO and FAC-ZnO were estimated according to Saers, method<sup>29</sup>. The obtained results are summarized in Table 1.

Table 1: Specific surface areas of single and composites materials

catalyst	ZnO	AC	FAC	AC-ZnO	FAC-ZnO
Specific surface area m <sup>2</sup> /g.	40	910	884	905	842

From these results, it is clear that AC shows high specific surface area this arises from its high porous structure and high content of vacancies. FAC shows relatively lower specific surface area this probably due to the effect of the presence of surface oxygenated groups. On the other hand it can be seen that, both of AC-ZnO and FAC-ZnO show remarkable reduction in surface area in comparison with AC and FAC. This can be attributed due to the strong interaction between the two solids AC and ZnO<sup>31,32</sup>.

### Powder X-rays diffraction (PXRD) for ZnO and AC/ZnO

XRD patterns of each of single and composite materials were investigated using powder X-rays diffraction. XRD patterns were recorded using Simadzu-6000 X-ray diffractometer with a nickel filter using monochromatized CuK $\alpha$  radiation at 40 kV and it was operated at 30 mA. These patterns are shown in Figures 3 and 4. From these figures it can be seen that, ZnO nanoparticles have a crystalline structure with characteristic peaks at 2 $\theta$  equal to 31.79, 34.45, 36.26, 47.33, 51.30, 56.26, 62.35, 65.84, 67.48, and 68.41.<sup>33,34</sup> The crystal size was calculated using Scherrer's equation and it was around 68 nm. For composite materials XRD patterns of AC-ZnO and FAC-ZnO are almost similar to that of neat ZnO. In general there was no change in XRD patterns for composites in comparison with XRD patterns of ZnO alone. This means that combination of AC and ACF with ZnO in the used ratio in this study (10%) doesn't affect the crystalline structure of ZnO.

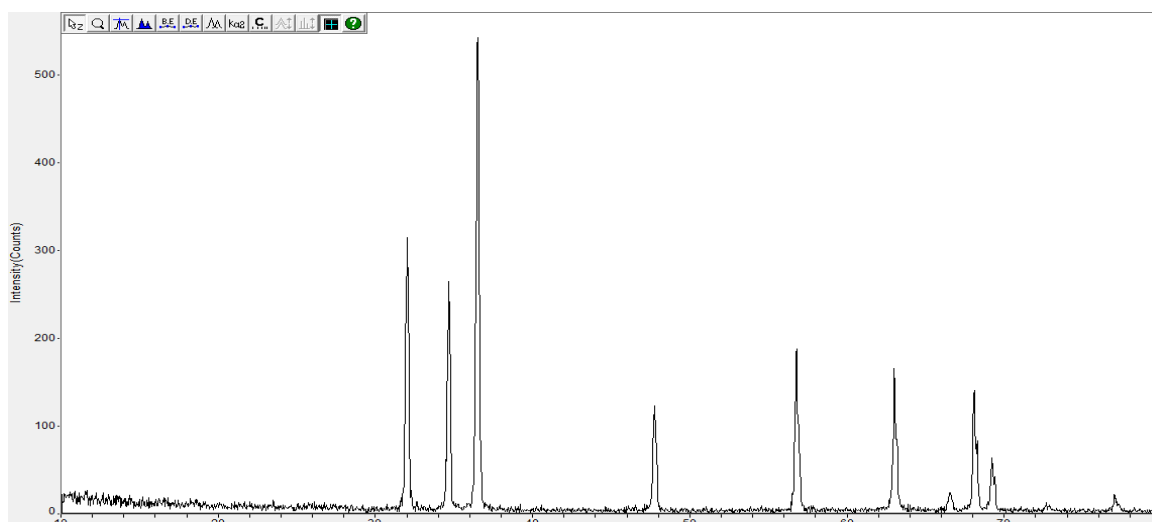


**Figure 3: XRD patterns for neat ZnO**

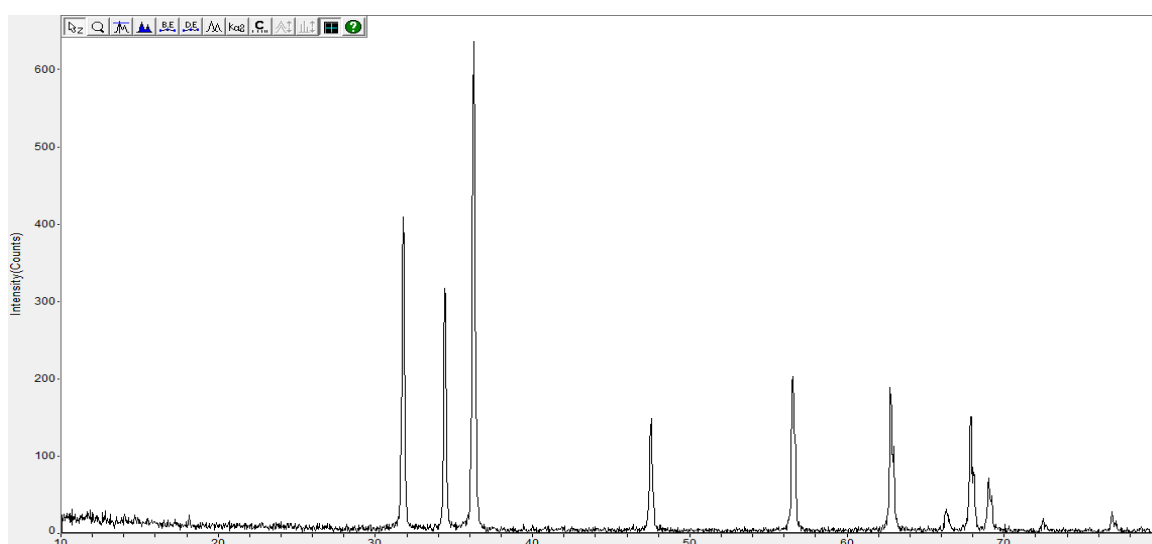


**Figure 4: XRD patterns of AC-ZnO and FAC-ZnO**

### Fourier transform infrared spectroscopy (FTIR)

The functional groups for AC and AC-ZnO were investigated using Perkin Elmer Spectrophotometer. FTIR spectra of AC and AC-ZnO are recorded from 400-4000  $\text{cm}^{-1}$  and are shown in Figure 5. FTIR spectra shows a peak around 3250-3550  $\text{cm}^{-1}$  which is assigned to the stretching vibration of OH group at the surface of zinc oxide. The peak in the range of 400-600  $\text{cm}^{-1}$  is assigned to the characteristic peak which related to (Zn-O) in the bulk zinc oxide<sup>35,36</sup>. In case of AC/ZnO and FAC/ZnO, these materials are in general show a broadening in FTIR spectra for ZnO framework region. For AC/ZnO sample, it can be seen that, a broadening in FTIR spectra for ZnO framework region was observed. Beside that it can be seen some peaks that are related to the AC in range of 1350 – 1710  $\text{cm}^{-1}$ . The band around 1600  $\text{cm}^{-1}$  which is assigned to C=O bond. The band around 1600  $\text{cm}^{-1}$  is related to the vibration mode of aromatic rings in coupling with carbonyl groups at the surface. The peak around 1000  $\text{cm}^{-1}$  is assigned to stretching modes of C=O bond. A weak broad band around 3000  $\text{cm}^{-1}$  is attributed to presence of C=C bonds. The band around 800  $\text{cm}^{-1}$  is related to vibration of the C-H bending mode. The bands around 2500  $\text{cm}^{-1}$  is assigned to stretching modes of hydroxyl groups. The bands around 3500 to 4000  $\text{cm}^{-1}$  are assigned to the stretching modes of surface hydroxyl OH groups<sup>37</sup>. For FAC/ZnO sample, FTIR spectra are similar to that of AC/ZnO and beside above peaks that were assigned for AC/ZnO it can be seen that, there are peaks located from 1000-1600  $\text{cm}^{-1}$  and these peaks are assigned to cyclic ether and quinone<sup>38</sup>.

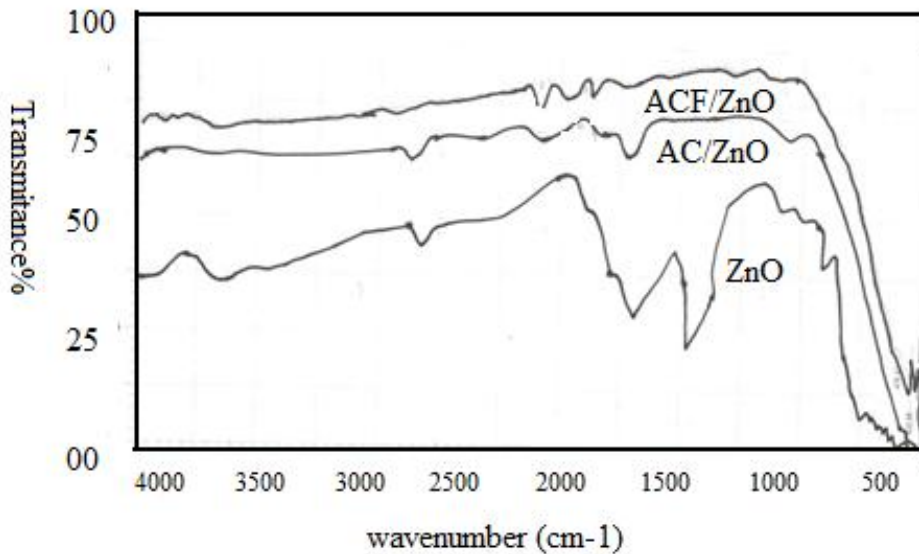


Figure 5: FTIR spectra of ZnO, AC/ZnO and FAC/Zn

#### Photocatalytic activity of single and composites materials

In order to investigate photocatalytic activity of each of AC, ZnO and AC-ZnO, a series of experiments were performed and these experiment were carried out in photoreactor that is shown in Figure 2. In all experiments, 0.05g. of the used materials were suspended in 30 mL of 50 ppm of CBB dye with continuous stirring under normal air conditions at 293 K. In all cases, dark reaction was conducted by stirring for 15 minute to reach adsorption equilibrium. Then photocatalytic reaction was initiated under illumination with UV light from low pressure mercury lamp. In this system, temperature was controlled at a desired value using a thermostatic circulation water jacket. The obtained results of photocatalytic removal of CBB dye over a suspension of each of single and composites materials are shown in Figure 6.

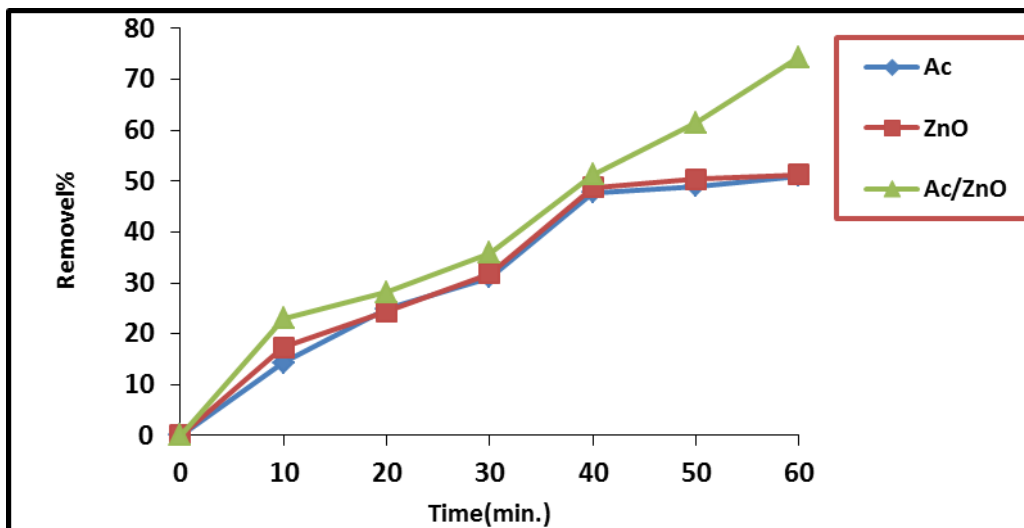


Figure 6: photocatalytic removal of CBB dye over single and composite materials.

From the presented results, it can be seen that the better removal efficiency of CBB dye after one hour of was obtained when use of AC-ZnO and around of 75% of dye was removed. This probably due to the synergistic effect of AC and ZnO, AC has high surface area which enable this composite system to offer high adsorption ability. Besides that, presence of AC particles in this composite can reduce recombination reaction between conduction band electrons ( $e^-_{CB}$ ) and valence band holes ( $h^+_{VB}$ ) by increasing separation between

these species<sup>39</sup>. In case of neat ZnO, the last process leads mainly to reduce the efficiency of the photocatalytic process. In case of AC-ZnO, these redox species would migrate to the surface and then participate in redox reactions with the pre-adsorbed species on the surface<sup>40</sup>.

### Optimizing of the used dosage of composite AC-ZnO materials

In order to investigate the effect of dosage of composite AC-ZnO on the photocatalytic removal of CBB dye over a suspension of supported zinc oxide a series of experiments were performed using different masses of AC-ZnO. In this study three different masses were used and these were 0.05, 0.10 and 0.15 g. In all experiments, a desired mass was suspended in 30 mL, 50 ppm at 293 K with continuous stirring under illumination with UV light from low pressure mercury lamp. The obtained results are presented in Figure 7.

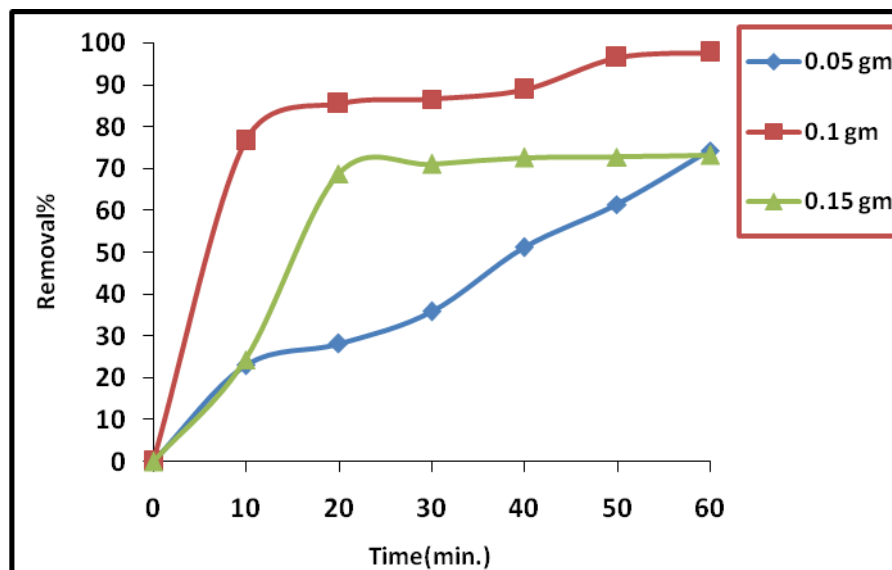


**Figure 7: Effect of dosage of AC-ZnO on photocatalytic removal of CBB over supported zinc oxide and irradiation with UV light at 293 K.**

From these results, it can be seen that the efficiency of dye removal was increase with increase of mass of AC-ZnO from 0,05 to 0.10 gram at 293 K and the efficiency of dye removal was around 98% after one hour of photocatalytic reaction under UV light. Increase in the efficiency of dye removal with increase of dosage can be attributed to the increase of active sites on the surface due to increase of number of particles. This would lead to absorb photons of light effectively according to first law of photochemistry. This arises to produce  $e_{CB}^-$  and  $h_{VB}^+$  effectively, these reactive species would contribute in redox reaction at the surface which results in dye removal with high efficiency<sup>41,42</sup>. Upon increasing the mass of catalyst more than 0.10 gram, the removal efficiency decrease at 0.15 g., this is due to the aggregation of the particles of catalyst and production of inner filter in the bulk mixture. This leads to scatter of photons of light from other part of mixture. According to this phenomenon, light would not absorb by all particles which leads to reduce the efficiency of generation of photoactive species<sup>43</sup>. The result of this effect leads to reduce the efficiency of dye removal at masses higher than 0.10 g. (c.a. 0.15 g.). So that the efficiency of dye removal was declined from 98% to 73% at mass dosage of AC-ZnO equal to 0.15 g.

### The effect of pH on the photocatalytic removal of CBB dye over AC-ZnO

To investigate the effect of pH of reaction mixture on the photocatalytic removal of CBB dye over a suspension of AC-ZnO, a series of experiments were performed using 0.10 g. of the material in 30 mL of dye solution (50 ppm) at 293 K under irradiation with UV light from low pressure mercury lamp. All experiments were carried out under the same reaction conditions, these experiments were performed at three different pHs, 3, 4 and 9. The obtained results of dye removal are presented in in Figure 8.

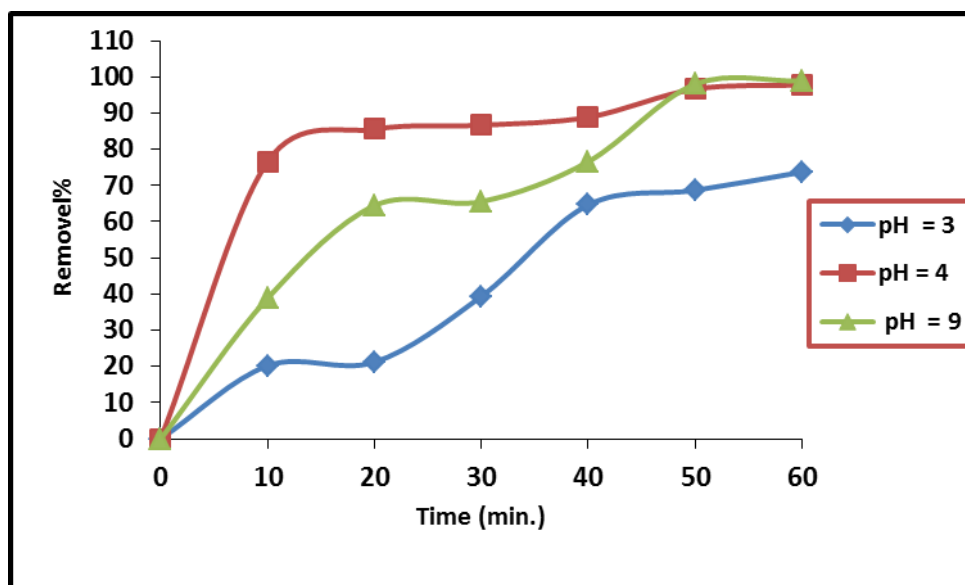


**Figure 8:Photocatalytic removal of CBB over AC-ZnO at different pH values**

From the above results, it can be seen that the efficiency of photocatalytic removal of CBB dye was increased with increase of pH into basic medium and the efficiency of dye removal reached to around 98% at pH=9. This effect can be attributed to enhance in adsorption of dye molecules over AC-ZnO surface<sup>44</sup>. This is an essential step in the photocatalytic reaction which leads to increase the efficiency of dye removal. On the other hand, acidic medium leads to increase repulsion between dye molecules and the surface which leads to reduce adsorption of dye molecule on the surface. This process results in reduction in the efficiency of dye removal under these circumstances.

#### **The effect of temperature on photocatalytic removal of CBB over AC-ZnO**

The effect of reaction temperature of the removal of CBB dye over a suspension of AC-ZnO under irradiation with UV light. A series of experiment were performed using same experimental arrangements at a range of temperature from 283- 303 K, a period of each run was one hour after dark reaction requirements. The obtained results are shown in Figure 9. From these results it can be seen that, the efficiency of dye removal was enhanced with elevation of reaction temperature from 283 up to 298 K. The better obtained removal efficiency was found at 298 K which was around 100%. After that, the removal efficiency was declined as temperature was further increased (303 K). These results can be attributed to the effect of temperature on the diffusion of dye molecules from bulk of the mixture on to the surface of the catalyst. Besides that, elevation in reaction mixture leads to increase concentration of active radical species, these species are contributed on redox reaction at the surface to cause further dye molecules fragmentation<sup>45,46</sup>. On the other hand, further increase of reaction temperature (higher than 298 K) can be attributed to the desorption of dye molecules away from the surface via gained extra kinetic energy that is obtained from thermal activation<sup>45,46</sup>.

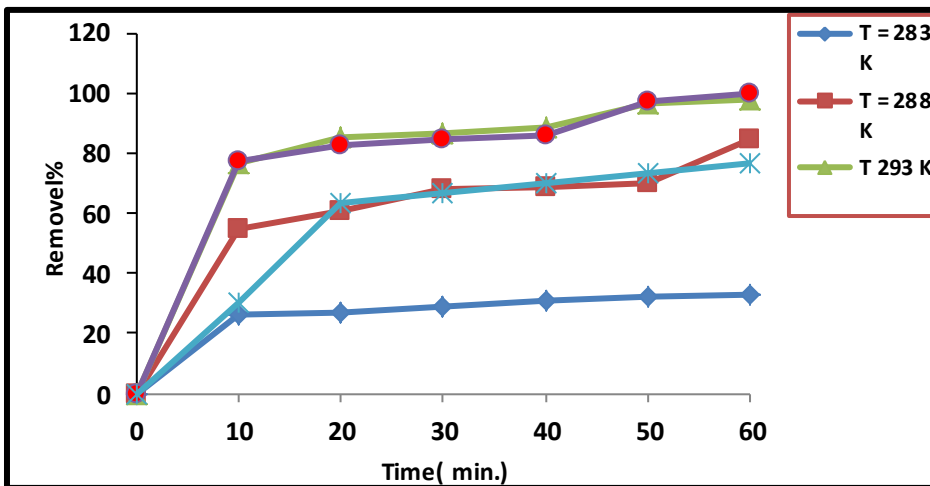


Figure 9: The effect of temperature of reaction mixture on dye removal over AC-ZnO.

**Calculation of activation energy for the photocatalytic removal of CBB dye over AC-ZnO**

Activation energy for the photocatalytic removal of CBB dye over a suspension of AC/ZnO was calculated according to Arrhenius equation by performing a series of experiments at 283, 288, 293 and 295 K<sup>47</sup>. Activation energy was calculated by plotting Ln k against 1/T as shown in Figure 10. From this plot, the activation energy was 27.71 kJ/mol. This results are agree with the values of activation energies for the photocatalytic reactions and it is mainly dependent on the energy required for transfer photogenerated species from the bulk of the photocatalyst into the surface to participate in redox reactions at the surface<sup>47</sup>.

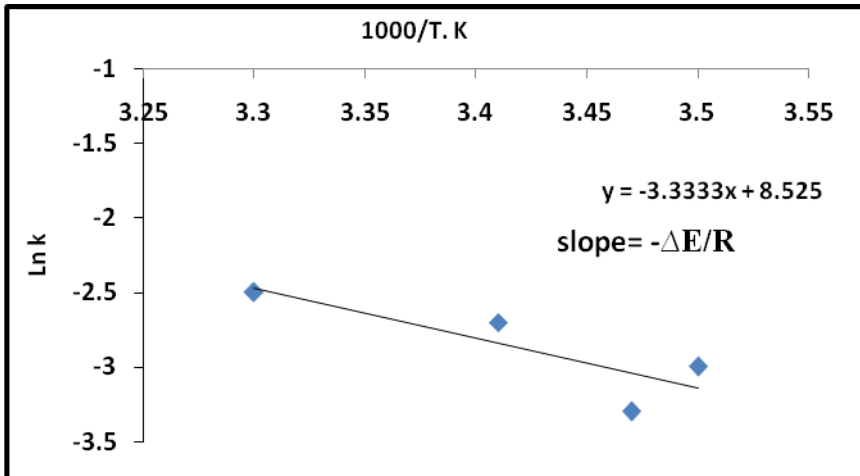


Figure 10: Arrhenius plot for the photocatalytic removal of CBB dye over AC-ZnO

**Photocatalytic activity of FAC-ZnO and AC-ZnO on CBB dye removal**

In order to investigated the photocatalytic activity for the functionalized AC and its combination with zinc oxide. A series of experiments were carried using 0.10 g. of both of FAC-ZnO and AC-ZnO in 30 mL of 50 ppm of dye solution at 293 K under UV radiation from low pressure mercury lamp. The obtained results are presented in Figure 11. From these results, it can be seen that AC-ZnO was more efficient than FAC-ZnO on cBB dye removal under the same rreaction conditions. This can be attributed to the role of functionalization of AC in repulsion of dye molecules with the surface as well as their role in light scattering away from the surface of FAC-ZnO<sup>48</sup>. These two factors can result in reduction of the photocatalytic activity of FAC-ZnO in comparison with AC-ZnO<sup>49,50</sup>.

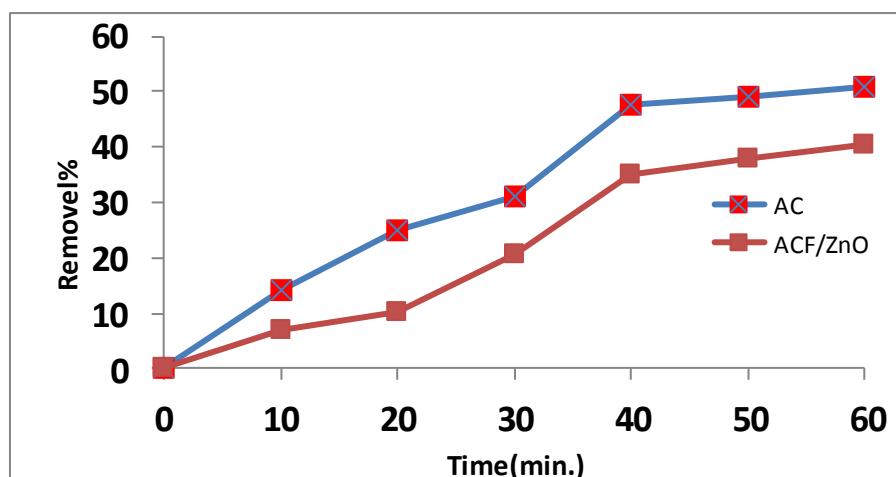


Figure 11: Photocatalytic removal of CBB dye over AC-ZnO and ACF-ZnO

## Conclusions

In this study a supported zinc oxide with both activated carbons and functionalized activated carbon were synthesized successfully. The obtained results showed that combination of AC with ZnO doesn't affect significantly on its crystalline structure as it was investigated from XRD patterns for each of ZnO and AC-ZnO. Also it was noted that the photocatalytic activity of ZnO was improved in case of supporting with AC rather than photocatalytic activity of neat ZnO.

## References

1. Wadood M., Hasan F., and Abbas M., Removal of Dyes from Wastewater of Textile Industries Using Activated Carbon and Activated Alumina, *Iraqi Journal of Chemical and Petroleum Engineering*, 2007, 9(4), 43-52.
2. Kansal, S.K.; Kaur, N. and Singh, S. Photocatalytic degradation of two commercial reactive dyes in aqueous phase using nanophotocatalysts. *Nanoscale Res. Lett.*, 2009, 4, 709–716.
3. Ling, L.C. Treatment of A Reactive Dye, A Disperse Dye, and Their Mixtures Using H<sub>2</sub>O<sub>2</sub>/Pyridine/Cu (II) System. M.Sc. Thesis submitted to University of Science, Malaysia. 2009.
4. Shaul, G.M.; Holdsworth, T.J.; Dempsey, C.R. and Dostal, K.A. Fate of water soluble azo dyes in the activated sludge process. *Journal of Chemosphere*, 1991, 22(1-2), 107-119.
5. Aljeboree AM, Alkaim, A. F., and Al-Dujaili, A. H. (2015); Adsorption isotherm, kinetic modeling and thermodynamics of crystal violet dye on coconut husk-based activated carbon. *Desalin. Water Treat.* 53(13): 3656-3667.
6. A. M. Aljeboree, A. N. Alshirifi, and A. F. Alkaim. (2014); Kinetics and equilibrium study for the adsorption of textile dyes on coconut shell activated carbon. *Arabian J. Chem.* 10.1016/j.arabjc.2014.01.020.
7. Amrin, A. R. Photocatalytic oxidation of congo red dye by using Co<sub>2</sub>O<sub>3</sub>-Cr<sub>2</sub>O<sub>3</sub> as a photocatalyst, *Mesop. Environ. J.*, 2016. 2 (2), 66-74.
8. Slokar, Y.M. and Marechal, M.L. Methods of decoloration of textile wastewaters. *Journal of Dyes and Pigments*, 1998, 37(4), 335-356.
9. Saïen, J. and Khezrianjoo S., Degradation of the fungicide carbendazim in aqueous solutions with UV/TiO<sub>2</sub> process: optimization, kinetics and toxicity studies. *Journal of Hazardous Materials*, 2008, 157(2-3), 269–276.
10. Hoffman, M. R.; Martin, S. T.; Choi, W. and Bahnemann, D. W. Environmental applications of semiconductor photocatalyst. *Chemical Reviews*, 1995, 95(1), 69–96.

11. Vincenzo Vaiano, , , Giuseppina Iervolino, Diana Sannino, Julie J. Murciab, Maria C. Hidalgo, Paolo Ciambellia and José A. Navío. Photocatalytic removal of patent blue V dye on Au-TiO<sub>2</sub> and Pt-TiO<sub>2</sub> catalysts. *Applied Catalysis B: Environmental*, 2016, 188(5), 134–146.
12. Ibhaddon, A.O. and Fitzpatrick, P. Heterogeneous photocatalysis: recent advances and applications. *Journal of Catalysts*, 2013, 3, 189-218.
13. Nakata K, and Fujishima A., TiO<sub>2</sub> photocatalysis: Design and applications. *Journal of Photochemistry and Photobiology C: Photochemistry Reviews*, 2012, 13(3), 169-89..
14. Priyanka and Srivastava V.C. Photocatalytic oxidation of dye bearing wastewater by iron doped zinc oxide. *Ind. Eng. Chem. Res.*, 2013, 52, 17790–17799.
15. Daneshvar, N.; Aber, S.; Seyed Dorraji, M. S.; Khataee, A. R., and Rasoulifard, M. H. Photocatalytic degradation of insecticide diazinon in the presence of prepared nanocrystalline ZnO powders under irradiation of UV-C light. *Sep. Purif. Technol.*, 2007, 58, 91–98.
16. Alkaim AF, Dillert R, Bahnemann DW. (2015); Effect of polar and movable (OH or NH<sub>2</sub> groups) on the photocatalytic H<sub>2</sub> production of alkyl-alkanolamine: a comparative study. *Environmental Technology*. 36(17): 2190–2197.
17. Pelizzetti, E. Concluding remarks on heterogeneous solar photocatalysis, *Sol. Energ. Mat. Sol. Cells*, 1995, 38, 453–457.
18. Sobana, N. and Swaminathan, M.; Combination effect of ZnO and activated carbon for solar assisted photocatalytic degradation of Direct Blue 53, *Sol. Ener. Mat. Sol. C.*, 2007, 91, 727-734.
19. Jiang, L.; and Gao, L.; Fabrication and characterization of ZnO-coated multi-walled carbon nanotubes with enhanced photocatalytic activity, *Mat. Chem. Phys.*, 2005, 91, 313-316.
20. Gokona, N.; Hasegawa, N.; Kaneko, H.; Aoki, H.; Tamaura, Y. and Kitamura, M., “Photocatalytic effect of ZnO on carbon gasification with CO<sub>2</sub> for high temperature solar thermochemistry, *Sol. Ener. Mater. Sol. C.*, 2003, 80, 335-341.
21. Rohe, B.; Veeman, W. S.; and Tausch, M.; Synthesis and photocatalytic activity of silane-coated and UV-modified nanoscale zinc oxide, *Nanotechnol.* 2006, 17, 277–282.
22. Kalpana, D.; Omkumar, K. S.; Kumar, S. S. and Renganathan, N.G.; A novel high power symmetric ZnO/carbon aerogel composite electrode for electrochemical supercapacitor”, *Electrochim. Acta.* 2006, 52, 1309-1315.
23. Cordero T, Duchamp C, Chovelon JM, Ferronato C, and Matos J., Surface nano-aggregation and photocatalytic activity of TiO<sub>2</sub> on H type activated carbons. *Appl Catal B: Environ.*, 2007; 73: 227-35.
24. Cordero T, Duchamp C, Chovelon JM, Ferronato C and Matos J., Influence of L-type activated carbons on photocatalytic activity of TiO<sub>2</sub> in 4-chlorophenol photodegradation. *J Photochem Photobiol. A: Chem.*, 2007; 191: 122-31.
25. Z. Wang, *Journal of Physics: Condensed Matter*, Zinc oxide nanostructures: growth, properties and applications, 2004, 16, 829-858.
26. Ahmed F. Halbus, Abbas J. Lafta, Zahra H. Athab and Falah H. Hussein, Adsorption of Reactive Yellow Dye 145 from Wastewater onto Iraqi Zahdy and Khestawy Date Palm Seeds Activated Carbons, *Asian Journal of Chemistry*; 2014, 26, , 167-172.
27. J. Matos, J. Laine, J.-M. Herrmann, D. Uzcategui and J.L. Brito, Influence of activated carbon upon titania on aqueous photocatalytic consecutive runs of phenol photomineralization, *Appl. Catal., B: Environ.*, 2007, 70, 461-469.
28. W. M. Ashri, W. Daud and A. H. Houshamnd, Textural characteristics, surface chemistry and oxidation of activated carbon, *Journal of Natural Gas Chemistry*, 2010, 19, 267–279.
29. Dada A., Olalekan A., Olatunya A., Dada O. Langmuir, Freundlich, Temkin, and Dubinin-Radushkevich, Isotherms studies of equilibrium sorption of Zn<sup>2+</sup> unto phosphoric acid modified rice husk, *Journal of Applied Chemistry*, 2012, 3(1), 38-45.
30. Ameri A., and Esrafiy A. Synthesis and properties of Fe<sub>3</sub>O<sub>4</sub>-activate carbon magnetic nanoparticles for removal of aniline from aqueous solution: equilibrium, kinetic and thermodynamic studies, *Iranian Journal of Environmental Health Sciences & Engineering*, 2013, 10(19), 1-9.
31. Hilal, H.S.; Majjad, L.Z.; Zatar, N.; and El-Hamouz, A.; Dye-effect in TiO<sub>2</sub> catalyzed contaminant photo-degradation: Sensitization vs. charge-transfer formalism”, *Solid State Sciences* 2007, 9, 9-15.
32. Rohe, B.; Veeman, W. S.; and Tausch, M.; Synthesis and photocatalytic activity of silane-coated and UV-modified nanoscale zinc oxide, *Nanotechnol.* 2006, 17, 277– 282.

33. C. S. Chen , T. G. Liu , L. W. Lin , X. D. Xie , X. H. Chen , Q. C. Liu , B. Liang , W. W. Yu, and C. Y. Qiu, 2013, Multi-walled carbon nanotube-supported metal-doped ZnO nanoparticles and their photocatalytic property, *J. Nanopart Res.*, 2013, 15, 2-9.
34. Seery M., George R., Floris P., Pillai S., Silver doped titanium dioxide nanomaterials for enhanced visible light photocatalysis, *J. Photochem. Photobiol. A: Chem.*, 2007, 189, 258-264.
35. Gunalan S., Sivaraj R., Rajendran V., Green synthesis of zinc oxide nanoparticles by aloe barbadensis miller leaf extract: Structure and optical properties, *Materials Research Bulletin*, 2011, 46(12), 2011, 2560–2566.
36. Taps A., Majewski P., Aldinger F., Chemical Preparation of Pure and Strontium-and/or Magnesium-Doped Lanthanum Gallate Powders, *J. Am. Ceram. Soc.*, 2000, 83(12), 2954-2960.
37. Abbas J. Lafta , Amed F. Halbus , Zahraa H. Athab , Ahmed M. Kaamil , Ahmed S. Hussein , Asad F. Qhat and Falah H. Hussein, Effects of Activators on Adsorption Ability of Reactive Yellow-145 Dye on Activated Carbon from Iraqi Zahdi Date Palm Seeds, *Asian Journal of Chemistry*; 2014, 26, (2014), 119-123,
38. Matos J., Laine J., Herrmann J., Uzcategoui D., Brito J. L., Influence of activated carbon upon titania on aqueous photocatalytic consecutive runs of phenols photomineralization, *Appl. Catal. B: Environ.*, 2007, 70, 461-469.
39. Rusheng Yuan, Rogngbo Guan, and Jingtang Zheng, Effect of pore size of TiO<sub>2</sub> -loaded activated carbon fiber on its photocatalytic activity, *Scripta Materialia*, 2005, 52, 1329-1334.
40. Ahmed M. Kamil, Falah H. Hussein, Ahmed F. Halbus, and Detlef W. Bahnemann, Preparation, characterization and photocatalytic applications of MWCNTs/TiO<sub>2</sub> composite, *International Journal of Photoenergy*, 2014, 2014, 2-9.
41. Sobana, N. ; and Swaminathan, M.; Combination effect of ZnO and activated carbon for solar assisted photocatalytic degradation of Direct Blue 53, *Sol. Ener. Mat. Sol. C.*, 2007, 91, 727-734.
42. Gokona, N.; Hasegawa, N.; Kaneko, H.; Aoki, H.; Tamaura, Y. .and Kitamura, M., Photocatalytic effect of ZnO on carbon gasification with CO<sub>2</sub> for high temperature solar thermochemistry, *Sol. Ener. Mater. Sol. C.*, 2003, 80, 335-341.
43. Rohe, B.; Veeman, W. S.; and Tausch, M.; Synthesis and photocatalytic activity of silane-coated and UV-modified nanoscale zinc oxide, *Nanotechnol.* 2006, 17, 277– 282.
44. Neppolian, B.; Choi, H. C.; Sakthivel, S.; Arabindoo, B.; and Murugesan, V. Solar/UV-induced photocatalytic degradation of three commercial textile dyes, *J. Haz. Mat.* 2002, 89, 303-317.
45. Hermann J. M., Heterogeneous photocatalysis: Fundamentals and applications to the removal of various types of aqueous pollutants, *Catal. Today*, 1999, 53, 115-129. 46. Robert D., Photosensitization of TiO<sub>2</sub> by M<sub>x</sub>O<sub>y</sub> and M<sub>x</sub>S<sub>y</sub> nanoparticles for heterogeneous photocatalysis applications, *Catal. Today*, 2007, 122, 20-26. .
46. A. Attia, S. Kadhim and F. Hussein, Photocatalytic Degradation of textile dyeing Wastewater using titanium dioxide and zinc oxide, *E-Journal of Chemistry*, 2008, 5(2), 219-223.
47. Pelekani C., and Snoeyink VL., A kinetic and equilibrium study of competitive adsorption between atrazine and Congo red dye on activated carbon: the importance of pore size distribution *Original, Carbon*, 2001, 39(1), 25-37.
48. Hsisheng T., and Sheng-Chi W. , Preparation of porous carbons from phenol-formaldehyde resins with chemical and physical activation, *Carbon*, 2000, 38(6), 817-824.
49. Li L., Quinlivan P., and Knappe D., Fibers to make them suitable for conversion into high performance carbon, *Carbon*, 2002, 40, 2805- 2809.

\*\*\*\*\*